J|A|C|S
ARTICLES
Published on Web 04/18/2006

Water Soluble Cryptophanes Showing Unprecedented Affinity for Xenon: Candidates as NMR-Based Biosensors

Gaspard Huber,[†] Thierry Brotin,[‡] Lionel Dubois,[†,§] Hervé Desvaux,[†] Jean-Pierre Dutasta,[‡] and Patrick Berthault*,[†]

Contribution from the Laboratoire Structure et Dynamique par Résonance Magnétique, DSM/DRECAM/Service de Chimie Moléculaire, URA CEA/CNRS 331, CEA/Saclay, F-91191 Gif sur Yvette, France, and Laboratoire de Chimie de l'ENS Lyon, UMR 5182 CNRS-ENS Lyon, Ecole Normale Supérieure de Lyon, 46, Allée d'Italie, F-69364 Lyon Cedex 07, France

Received January 13, 2006; E-mail: pberthault@cea.fr

Abstract: Cryptophanes bearing OCH_2COOH groups in place of the methoxy groups represent a new class of xenon-carrier molecules soluble in water at biological pH. By using ^1H and ^{129}Xe NMR (thermally- and laser-polarized dissolved gas), the structural and dynamical behaviors of these host molecules as well as their interaction with xenon are studied. They are shown to exist in aqueous solution under different conformations in very slow exchange. A saddle form present for one of these conformations could explain the ^1H NMR spectra. Whereas the cryptophanes in such a conformation are unable to complex xenon, unprecedented high binding constants are found for cryptophanes in the other canonical crown−crown conformation. These host molecules could therefore be valuable candidates for biosensing using ^{129}Xe MRI.

I. Introduction

Xenon 129 is a promising isotope for surface or in vivo MRI. First, the deformation capabilities of its electronic cloud induce a large chemical-shift dependence on the molecular environment. Second, its nuclear magnetization can be polarized through optical pumping, which leads to a very high NMR sensitivity.

Cryptophanes are known to exhibit strong affinity for small neutral molecules. In the aim of conceiving a powerful biosensing system based on laser-polarized xenon MRI,[1,2] the design of cryptophane derivatives soluble in water is of crucial importance. They will constitute the hydrophobic core designed to capture the noble gas and on which a recognition antenna will be grafted. Their expected properties are strong binding of the noble gas atom and large chemical shift variation between bound and free xenon. The latter effect offered by the aromatic cage can open access to chemical shift imaging through net differentiation of the resonance frequencies of xenon free in solvent and xenon bound to the host. Moreover, these cage molecules should be rather soluble in water and in blood in a biological pH range, and in a second step, their toxicity must be assessed.

Only cryptophane-A,[3] cryptophane-E,[4] and cryptophane-O,[4] bearing 2, 3, and 5 CH_2-groups on their alkoxy linkers, respectively, had been modified so far to provide water-soluble hosts. The replacement of their methoxy groups by OCH_2COOH groups enabled solubilization of the resultant molecules at pH > 5. In the purpose of xenon binding, however, according to the results in organic phase for the "native" cryptophanes,[5] the two latter cages seem too big to tightly encapsulate xenon. Hence, Brotin et al.[5] have shown that the affinity of these host molecules for xenon is directly related to the size of the cage, the strongest affinity being found for cryptophane-A. Consequently, by analogy, it seemed judicious to study the structural and dynamical features of the binding of xenon inside new hosts issued from cryptophane-A (equivalent to cryptophane-222, **1**), cryptophane-223 (**2**), cryptophane-233 (**3**), and cryptophane-E (equivalent to cryptophane-333, **4**). To minimize the xenon relaxation through dipolar interaction with surrounding protons, a partially deuterated water-soluble cryptophane-A has also been synthesized (**5**). All of these cryptophanes are represented in Figure 1. Besides the fundamental interest for the understanding of molecular recognition solely based on van der Waals forces, the key idea behind this work is the design of xenon-carrier molecules of different types, resulting in very different xenon chemical shifts. Such hosts could consequently be used jointly in biosensing in a multiplexed way, different cages with different tethers recognizing different receptors in the same solution.

The present paper uses thermally polarized or laser-polarized xenon in a comparative study of host−guest interactions for xenon inside these water-soluble cryptophanes. Such a study begins with an analysis of the structure and the conformation

[†] Laboratoire Structure et Dynamique par Résonance Magnétique.
[‡] Laboratoire de Chimie de l'ENS Lyon.
[§] Present address: Service de Chimie Inorganique et Biologique, 17 avenue des Martyrs, CEA/Grenoble, 38054 Grenoble, France.

(1) Spence, M. M.; Rubin, S. M.; Dimitrov, I. E.; Ruiz, E. J.; Wemmer, D. E.; Pines, A.; Qin Yao, S.; Tian, F.; Schultz, P. G. *Proc. Natl. Acad. Sci. U.S.A.* **2001**, *98*, 10654−10657.
(2) Spence, M.; Ruiz, E.; Rubin, S.; Lowery, T.; Winssinger, N.; Schultz, P.; Wemmer, D.; Pines, A. *J. Am. Chem. Soc.* **2004**, *126*, 15287−15294.
(3) Canceill, J.; Lacombe, L.; Collet, A. *J. Chem. Soc., Chem. Commun.* **1987**, 219−221.
(4) Garel, L.; Lozach, B.; Dutasta, J.; Collet, A. *J. Am. Chem. Soc.* **1993**, *115*, 11652−11653.
(5) Brotin, T.; Dutasta, J.-P. *Eur. J. Org. Chem.* **2003**, 973−984.

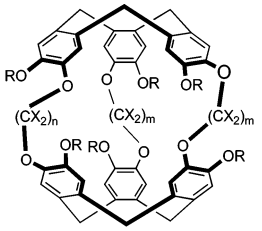

1; R = CH_2COOH; X = H; m= 2 ; n = 2
2; R = CH_2COOH; X = H; m= 2 ; n = 3
3; R = CH_2COOH; X = H; m= 3 ; n = 2
4; R = CH_2COOH; X = H; m= 3 ; n = 3
5; R = CD_2COOH; X = D; m= 2 ; n = 2

Figure 1. Generic structure of the cryptophane derivatives under study. In the text, a comparison is made with their organic analogues (R=CH_3, X=H): **6**: $m = 2$, $n = 2$; **7**: $m = 2$, $n = 3$; **8**: $m = 3$, $n = 2$; **9**: $m = 3$, $n = 3$.

of these host molecules in aqueous solution, on the basis of the observation of ^{1}H NMR data.

II. Results and Discussion

A. Structure and Dynamics of the Water-Soluble Cryptophanes. The ^{1}H NMR spectra of **1**−**4** display more peaks than a priori expected from their canonical structure. For instance, only two aromatic signals are expected for cryptophanes of D_3 symmetry (**1** and **4**); these correspond to the two inequivalent protons on the aromatic rings that are all equivalent. On a degassed sample, the low-field region of the ^{1}H NMR spectrum of **1** exhibits not only these two main peaks, but also twelve smaller signals of similar intensity. It is likely that in addition to the canonical form, **1** can exist under asymmetric conformations. Non canonical forms are also observed on the ^{1}H NMR spectra of cryptophanes **2**−**4** (not shown).

The presence of a peculiar conformation for cryptophane **4** would not be really surprising, because it has been previously observed that the parent molecule (cryptophane-E, **9**) is able to adopt a conformation such that one of the two cyclotriveratrylene units is inverted, passing from a convex to a concave form.[6] This conformation is known to appear in the solid state, when the encapsulated solvent is stripped off upon heating, or under strong degassing conditions. Also, Collet and co-workers have reported the presence of such in−out topoisomers for bigger syn and anti cryptophanes.[7] Even though this topoisomery could justify the presence of additional proton signals for **4**, such an explanation is not satisfactory for **1**, **2**, and **3** because of steric hindrance.

However, since the 80's, the presence of different isomers for cyclotriveratrylene (CTV) units with various substitutions was evidenced.[8] Only recently has a saddle form been isolated.[9] It is obtained by a 180° rotation of one of the dihedral angles linking two aromatic units. Even for a compound with nonbulky substituents, such as depicted in Figure 2, the crown−saddle isomerization half-life at room temperature is longer than 1 day. Each aromatic or methylene proton signal in the crown form is split into several signals in the saddle form due to a break of symmetry. In the presence of bulky substituents, saddle conformers of CTVs have been shown to be stabilized (enthalpic factor), and the crown/saddle interconversion is slowed.[10]

Cryptophanes can be considered as substituted CTVs, where the substituent is attached in three points of the CTV, which is therefore less flexible. A neutral *exo*-ester-functionalized *m*-xylyl bridged cryptophane has recently been characterized by NMR and X-ray crystallography.[11] As for the aforementioned CTVs, this cryptophane exists in two forms. In the first one, the molecule presents a D_3 symmetry, both CTVs adopting a crown conformation (**CC** form). In the second one, one CTV adopts a crown conformation and the other one an asymmetric saddle conformation (**CS** form). The isomerization half-time between these two forms is about 5 days at 20 °C.

Here, for the water-soluble cryptophanes **1**−**3**, if full inversion of the CTV motif is improbable due to steric constraints, the presence of several additional aromatic peaks could arise from the presence of saddle forms for one of the two CTV units (**CS** form). In such a conformation, a methylene group bridging two aromatic rings points toward the interior of the cavity. To check that the observed chemical shift variations in **1** are due to this crown−saddle isomerization, the influence of ring current effects on proton chemical shifts has been assessed through simulations, considering that the simultaneous presence of a saddle form for both CTV units is also unrealistic. The CH_2 protons pointing toward the interior of the cavity for the saddle part of the **CS** conformer are strongly upfield shifted and should correspond to the signals at 0.1 and 2.1 ppm. There are two types of aromatic protons: those ortho to an ethyleneoxy linker and those ortho to a OCH_2COOH group. Considering the two inequivalent CTV units in the **CS** form, it is therefore expected that the saddle−saddle exchange of one CTV will affect four different peak families (two for the saddle CTV, two for the crown CTV). Given the lack of symmetry in the **CS** form, three positions will be available for each of these families, thus explaining the 12 aromatic signals appearing in addition to the signals of the **CC** form.

The computed ring current effects for the **CC** and **CS** conformations are self-consistent and compatible with the observed proton chemical shifts. The correlation coefficient on the CTV protons (i.e., without the ethylenedioxy linker protons) is 0.94. The largest deviation occurs for one of the two aromatic protons upfield shifted: it certainly reveals the limits of our simplistic model. Figure 3 displays the average structure of the **CS** form of cryptophane **1**.

As far as we know, such a crown−saddle isomerization effect has never been reported, except for cryptophanes with long linkers in organic solvents.[11] Such a situation, observed in aqueous solvent, could represent a track toward the understanding of host−guest recognition processes, via the study of host nuclei on such model compounds. Undoubtedly, external effects such as nature of the solvent, presence of dissolved gases, temperature, etc. are key factors acting on this equilibrium. Strong helium bubbling during several hours enables the recovery of nearly 100% of the **CC** form. Also, pressurization of the NMR sample with ~4 bar of xenon during several days at room temperature significantly modifies the **CC**/**CS** propor-

(6) Lozach, B.; Ph.D. Thesis, University of Lyon 1, 1991.
(7) Garcia, C.; Aubry, A.; Collet, A. *Bull. Soc. Chim. Fr.* **1996**, *133*, 853−867.
(8) Collet, A.; Gabard, J. *J. Org. Chem.* **1980**, *45*, 5400−5401.
(9) Zimmermann, H.; Tolstoy, P.; Limbach, H.-H.; Poupko, R.; Luz, Z. *J. Phys. Chem. B* **2004**, *108*, 18772−18778.
(10) Zimmermann, H.; Bader, V.; Poupko, R.; Wachtel, E. J.; Luz, Z. *J. Am. Chem. Soc.* **2002**, *124*, 15286−15301.
(11) Mough, S. T.; Goeltz, J. C.; Holman, K. T. *Angew. Chem., Int. Ed.* **2004**, *43*, 5631−5635.

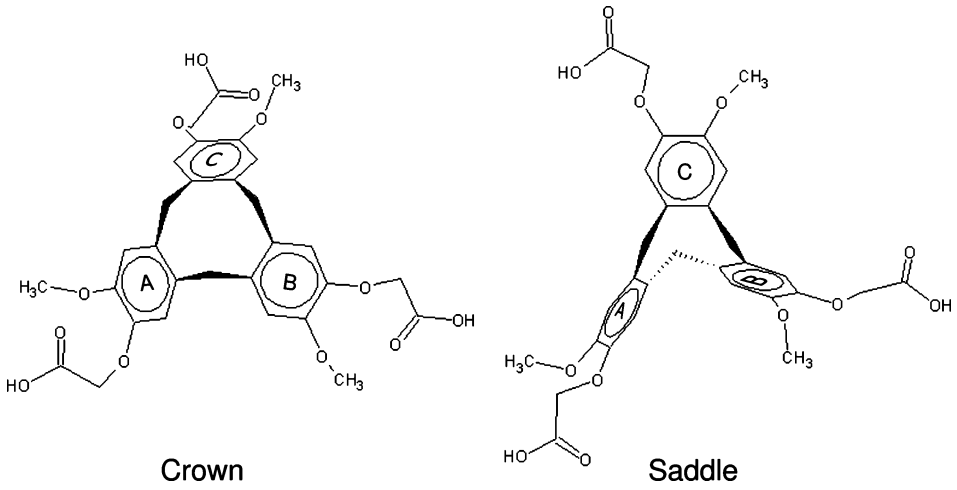

Figure 2. Isomerization of a cyclotriveratrylene unit.

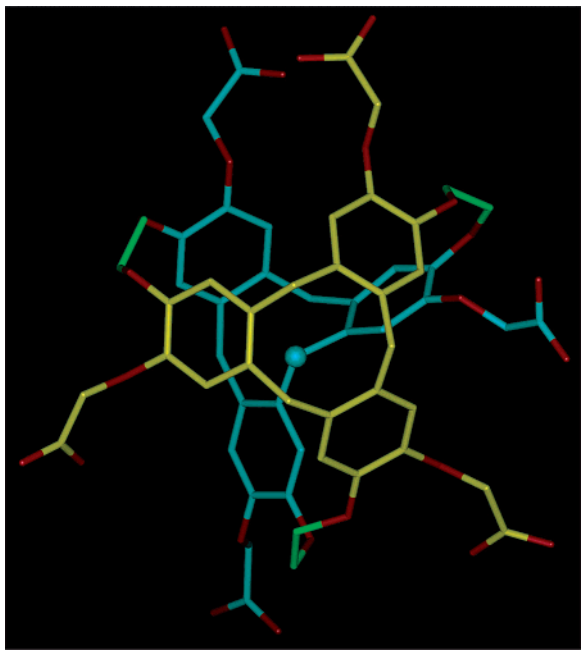

Figure 3. Average structure of the **CS** form of cryptophane **1**. Only the (+) enantiomer is shown. For sake of simplicity, the hydrogens are not displayed; the CTV unit in crown conformation is colored in yellow, the CTV unit in saddle conformation in cyan, and the alkoxy linkers in green. The carbon of the CH_2 bridge pointing toward the interior of the cavity is represented by a cyan sphere.

tion in favor of the former conformation but very slowly. A sample of **1** (pH 5.3, under air) was conserved in the dark at room temperature. In a time scale of about one week, the **CC** conformation almost disappears and the cryptophane adopts a **CS** conformation, as observed on the ^{1}H NMR spectrum. In such conditions, the **CS** form thus seems to be thermodynamically the most stable one. As we do not believe that the change from methoxy to OCH_2COOH groups can be taken for responsible of such an effect, the presence of these saddle forms might originate from a solvent effect. For cryptophanes **6**−**9** in tetrachloroethane, only tiny peaks representative of the **CS** form can be observed on the ^{1}H NMR spectra (not shown). Intuitively, due to the molecular size of tetrachloroethane, which has been reported as unable to enter in the cavity of cryptophane-A,[12] it

(12) Collet, A. *Tetrahedron* **1987**, *43*, 5725−5729.

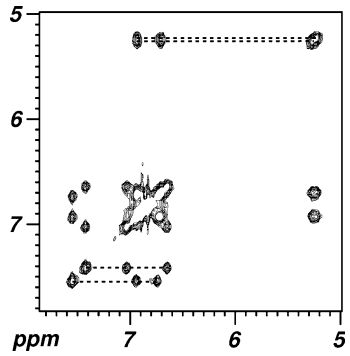

Figure 4. Expansion of the aromatic region of the EXSY contour plot for cryptophane **1**. Mixing time: 20 ms; temperature: 323 K. The dotted lines correspond to the four families of three peaks. In each family, an aromatic proton signal is exchanged to one of the two others after a saddle−saddle interconversion.

is hard to conceive that the saddle form cannot appear in such a solvent. Also, our results are in complete disagreement with the conclusions of Zimmermann et al.,[9] which state that the saddle form is disfavored in more polar solvents. The hydrophobic character of the cavity could be responsible for this difference of behavior. When water is the solvent, the cavity of the cryptophane under the **CC** form could be filled by a few ordered water molecules, which is entropically unfavorable. The cryptophane can, therefore, adapt itself to expel the water molecules by adopting a **CS** conformation.

Whereas the energy barrier for the **CC**−**CS** isomerization is very high and, thus, very difficult to measure, the **CS**−**CS** interconversion is faster and can directly be observed in the proton NMR spectra. A two-dimensional exchange spectroscopy (2D EXSY) experiment, of which the aromatic region is displayed in Figure 4, reveals the 12 small peaks, aforementioned 4 families of 3 signals, in slow exchange at the proton chemical-shift time scale. With this experiment, it becomes possible to extract the kinetics of the **CS**−**CS** interconversion. At 298 K, the exchange rate is measured at 2.30 ± 0.02 s^{-1}. From the **CS**−**CS** exchange rates measured at different temperatures between 273 and 323 K, the activation energy has been extracted: $E_a = 79.1 \pm 0.4$ kJ mol^{-1}. This activation barrier is 8 times higher than that observed for the isomerization of a CTV nona-substituted by bulky and lengthy $-OC(O)C_7H_{15}$ groups[10] in dimethyl formamide. The crown CTV exerts a strong constraint on the saddle CTV in **1**. However, relatively easily,

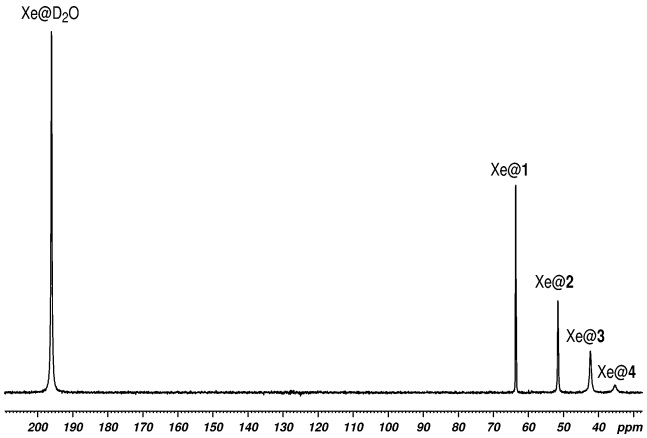

Figure 5. ^{129}Xe NMR spectrum of xenon in a D_2O solution containing a mixture of compounds **1** (0.74 mM), **2** (0.5 mM), **3** (0.69 mM), and **4** (0.69 mM). Spectrometer magnetic field: 11.7 T (138.36 MHz for the ^{129}Xe Larmor frequency), temperature: 289 K, partial pressure of xenon in natural isotopic abundance above the solution: 101 kPa.

a saddle form with, let's say, the dihedral angle between rings *A* and *B* inverted can be transformed in another saddle form where the dihedral between *A* and *C* is inverted simply by rotation of the methylene group situated between *A* and *C* (see Figure 2). The high-energy intermediate form might, thus, be a cryptophane where one of the cyclotriveratrylene units possesses two methylene bridges pointing toward the interior of the cavity. The high rigidity of the crown CTV does not seem to impede crown−saddle interconversion. At 298 K, it takes few days, corresponding to an activation energy of ca. 105 kJ/mol, less than for the nona-substituted CTV (activation energy of 115 kJ/mol). The rate is still lower than that observed for CTV substituted by methoxy groups, for which the interconversion takes about 5 h.[10] This may hardly be explained by the molecule structures themselves. The solvent and other minor species may play a role in this interconversion dynamics.

B. Properties of Cryptophanes 1−4 for Xenon Biosensing Applications. To evaluate the potential of these water-soluble cryptophanes for biosensing approaches using laser-polarized xenon NMR, four of their properties have been examined: (i) the chemical shifts of bound xenon (important parameter if combined use of several hosts is wished), (ii) their affinity for xenon, (iii) the kinetics of the binding, and (iv) the nuclear polarization lifetime of xenon in these cryptophanes.

1. Xenon Chemical Shifts. The use of dissolved, laser-polarized xenon enables a first snapshot of the ^{129}Xe NMR spectrum of a mixture of the four cryptophanes in D_2O, displayed in Figure 5. With respect to the signal of xenon in water at 197 ppm, the other signals corresponding to encapsulated xenon are upfield shifted. The xenon polarization, 4 orders of magnitude higher than the thermal one, enables the use of small quantities of dissolved gas, therefore leading to narrower lines for the bound signal.[13] Another advantage of using low gas concentration is that otherwise, xenon hydrates can form easily (above 12 bar at 20 °C, 4 bar at 10 °C),[14] impeding quantitative interpretation of the observed effects. Also, in the aim of measuring high binding constants, conditions where the xenon concentration is close to the host concentration are optimal. As previously observed for their congeners soluble in organic solvents (**6**−**9**), slow exchange conditions on the xenon chemical-shift time scale are observed for cryptophanes **1**−**4**. The chemical shift region for bound xenon is this of the noncondensed environment typical of cryptophanes.[15]

Table 1. ^{129}Xe Chemical Shifts in ppm Relative to the Gas Signal at Zero Pressure for Compounds **1**−**4** in Water or Their Parents **6**−**9** in 1,1,2,2-tetrachloroethane-d2, at 293 K

	Xe@ 222-cage	Xe@ 223-cage	Xe@ 233-cage	Xe@ 333-cage
Water-soluble cages (**1**−**4**, this work)	64	52	42	35
Organic cages (**6**−**8**: ref 5; **9**: ref 1)	68	60	47	30

As for the cryptophanes **6**−**9** in organic solvents, the xenon chemical shift decreases from **1** to **4**, i.e., with increasing cavity size. The chemical shifts of xenon in **1**−**4** at 293 K in D_2O have been compared to the corresponding series of xenon in organic cryptophanes (**6**−**9**) at the same temperature in 1,1,2,2-tetrachloroethane-d2 (see Table 1). Without entering into details, the chemical-shift increments inside a series are similar to those observed for the organic cryptophanes, confirming the preponderant role of the cavity size.[5,15] Also, as tetrachloroethane is supposedly unable to enter into the cryptophane cavity of **6**−**8**, the present correlation suggests that for **1**−**3**, the cavity of the water-soluble cryptophane cannot simultaneously contain a xenon atom and a water molecule. This is maybe not the case for **4**, where the xenon chemical shift higher and the peak sharper than for **9** could be explained by the presence of a water molecule reducing the cavity size and slowing down the xenon in−out exchange.

2. Kinetics of the Xenon Binding. Broadening of the ^{129}Xe peaks due to magnetic field and temperature inhomogeneity affects all the signals in the same way. The xenon line broadening due to field inhomogeneity has been estimated to ∼20 Hz on a pure D_2O sample. This rather high value arises from our experimental protocol: due to the transient nature of the xenon polarization, the spectra are recorded a few tens of seconds after shaking, leaving little time for complete homogeneity recovery. In the mixture of the four protonated water-soluble cryptophanes, the relative line widths are indicative of the various residence times of xenon in different environments. Indeed, the presence of different binding sites in large cryptophanes giving rise to the line broadening is not realistic as such a situation would imply high-energy barriers. Furthermore, when lowering the temperature to 275 K, the spectra still reveal only one peak for xenon in cryptophane, becoming sharper and sharper (not shown). This is a strong indication that line broadening does not arise from any exchange inside a cage but rather from the in−out exchange. The xenon exchange rates extracted from the line widths have thus been evaluated to 3.2, 11, 37, and 90 s^{-1} for **1**, **2**, **3**, and **4**, respectively, at 289 K under a xenon pressure of 101 kPa xenon. Given the low precision on the inherent line width of 20 Hz, these values are only indicative. However, the pairwise line-width differences are directly related to the change in the corresponding exchange rates. As for the native cryptophanes in organic solvent, the

(13) Huber, J. G.; Dubois, L.; Desvaux, H.; Dutasta, J.; Brotin, T.; Berthault, P. *J. Phys. Chem. A* **2004**, *108*, 9608−9615.
(14) Ohgaki, K.; Sugahara, T.; Suzuki, M.; Jindai, H. *Fluid Phase Equilib.* **2000**, *175*, 1−6.
(15) Sears, D. N.; Jameson, C. J. *J. Chem. Phys.* **2003**, *119*, 12231−12244.

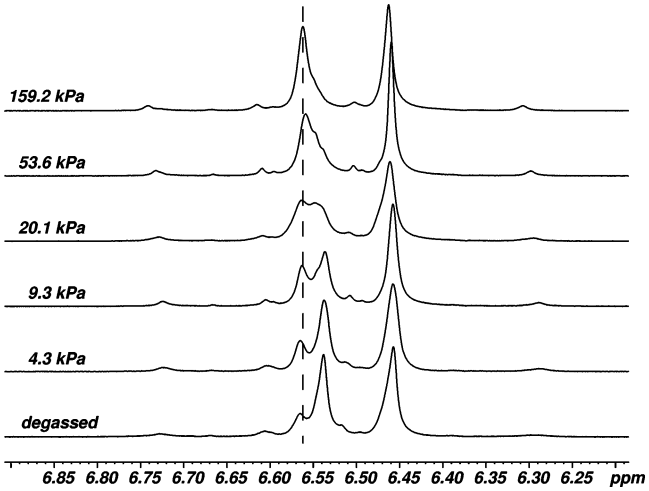

Figure 6. Aromatic region of the ^{1}H NMR spectrum of **4** (2.8 mM) with various xenon pressures indicated on the left of the spectra. Larmor frequency: 500.13 MHz; temperature: 293 K. The residual signal at 6.56 ppm present in the degassed sample is assigned to minor conformers of **4**, noninfluenced by xenon addition. This peak is connected in a NOESY experiment to the signal at 6.73 ppm, whose intensity is not modified upon xenon addition.

line width of bound xenon signal increases (the residence time of xenon inside the cavities decreases) from **1** to **4**, i.e., for increasing cavity size. The length and the flexibility of the alkylenedioxy linkers are responsible of such an effect.

At lower pressure, when the signal of free xenon in water is not observable, the line widths indicate a situation where almost no exchange is observed. It was indeed previously demonstrated that the collision mechanism between cryptophanes does not significantly contribute to the exchange process, as exemplified for **6** in 1,1,2,2-tetrachloroethane.[16] No coalescence effect has been observed for all cryptophanes **1**−**4** until 310 K under 101 kPa, conversely to the case of **6**−**9** in 1,1,2,2-tetrachloroethane. All the xenon peaks are perfectly distinguishable, even at this temperature. The sharp peaks observed at low pressure, therefore in conditions close to the experiment using laser-polarized gas, render optimistic for the final goal of the approach. These observations constitute an undeniable advantage for the biosensing applications using xenon chemical-shift imaging.

3. Estimation of the Binding Constants. An accurate estimation of the xenon−cryptophane binding constants appears to be much more complicated than in organic solvents,[13] due to the presence in solution of cryptophanes in **CS** conformation. The **CS** conformations have proton signals that evolve with xenon addition neither in chemical shift nor in intensity. This seems to indicate that these conformers are unable to bind xenon, which is supported by the presence of only one peak per cryptophane on the xenon spectra. Indeed, a situation where slow exchange on the proton chemical-shift time scale coexists with fast exchange on the xenon chemical-shift time scale is highly improbable, due to the relative range of chemical shifts. The proton spectra of **3**−**4** are significantly modified upon xenon addition. For example, Figure 6 for **4** indicates a change of the intensity ratio of the two lines at 6.53 and 6.56 ppm. We have assumed that the peak at 6.56 ppm is characteristic of the cage containing one xenon atom, and the peak at 6.53 ppm is characteristic of the xenon-free cage. From the respective area of these peaks as a function of the xenon pressure, extraction of the binding constants becomes possible for **3** and **4** (see Table 2).

Table 2. Computed Binding Constants (M^{-1}) for Xenon in Cryptophanes **1**−**4** in D_2O at 293 K

	xenon spectra		proton spectra	
sample	median value	90% confidence limits	median value	90% confidence limits
1	6800	5600−9100	n.m.[a]	n.m.[a]
2	2200	1800−2600	n.m.[a]	n.m.[a]
3	2200	1200−50000	1600	700−3500
4	1000	600−2900	920	280−2200

[a] n.m. = Not measured.

As only signals characteristic of the **CC** structure are used for calculation of the binding constants via the proton spectra, the presence of **CS** cryptophanes has no influence. On the contrary, they must be taken into account for the determination of the binding constant via xenon spectra. The first step is the estimation of the percentage of cages able to receive xenon, which is sample dependent but measurable on the proton spectra. Previous experiments have revealed that the **CS**−**CC** proportion is slowly modified by gas bubbling, and our protocol for dissolution of xenon should not displace this proportion. With these corrections, binding constants can be determined from the relative integration of the signals of free and bound xenon and the use of the model described in Materials and Methods. Their values are reported in Table 2.

A good agreement is observed between the two approaches. The highest binding constant occurs for xenon in **1**. The binding constant value decreases when the size of the cavity increases, as for the organic analogues. To the best of our knowledge, the binding constant value for **1** is the highest ever measured for a complex based only on van der Waals interactions in water. Also, it is remarkable that the complex is even stronger (by about a factor 2) than that between xenon and cryptophane-A in 1,1,2,2-tetrachloroethane at 278 K. This surely arises first from the lower solubility of xenon in water than in organic solvents. Second, unfavorable entropy of water inside the cages could have an important role on the resulting binding constants.

4. Xenon T_1. To test the feasibility of the biosensing experiment with these cage molecules, where the capability of the host to bind xenon must be accompanied by a conservation of the maximum of guest polarization, **5**, which is **1** deuterated on the ethylenedioxy linkers and on the OCH_2COOH groups, has been synthesized (24 nonlabile hydrogens have been replaced by deuterium atoms). In this way, the dipole−dipole relaxation from xenon to these nuclei should be assessed.

As seen on a laser-polarized ^{129}Xe spectrum of a mixture of both cryptophanes (shown in Supporting Information), the chemical shifts of xenon (110 kPa above the solution) in **1** and in **5** differ by ∼1 ppm. This chemical-shift-splitting value is similar to that afforded by partial deuteration of cryptophane-A in 1,1,2,2-tetrachloroethane-d2 at 238 K, showing the same influence of the isotopic substitution.[16,17]

Using laser-polarized noble gas, and NMR experiments consisting of a succession of small angle read pulses at constant

(16) Brotin, T.; Lesage, A.; Emsley, L.; Collet, A. *J. Am. Chem. Soc.* **2000**, *122*, 1171−1174.

(17) Brotin, T.; Devic, T.; Lesage, A.; Emsley, L.; Collet, A. *Chem.−Eur. J.* **2001**, *7*, 1561−1573.

time intervals, the following longitudinal relaxation times T_1 have been measured at 293 K for samples of concentration 3.9 mM at a proportion of 53% of filled cryptophane: 22.2 ± 2.0 s for **1**, 32.0 ± 0.9 s for **5**. It has been considered that $1/T_1$ is far slower than the in−out exchange rate. From these values, and considering a xenon T_1 value in the absence of cryptophane of 440 s (value in pure D_2O[18]), the relaxation times of encapsulated xenon are calculated to 12.1 and 17.6 s for **1** and **5**, respectively. It has also been checked that the xenon binding constant is the same for **1** and **5**, thanks to a ^{129}Xe spectrum of an equimolar mixture of these cryptophanes (see Supporting Information).

This reveals that the host−guest dipole−dipole interactions for the 24 involved nuclei contributes 31% of the total relaxation. The significant gain in relaxation time afforded by the partial deuteration of the host is a good indication on what could be undertaken to lengthen the lifetime of the hyperpolarization. In light of previous xenon−proton magnetization transfer experiments on cryptophanes,[19] a further increase of the xenon relaxation times would arise from deuterium labeling of the aromatic rings. For instance, using the proton−xenon cross-relaxation-rate ratios extracted by Luhmer et al.[20] from SPINOE experiments on cryptophane-A, a rough approximation leads to an expected xenon T_1 multiplied roughly by 2.5 for a fully deuterated cryptophane.

III. Materials and Methods

A. Synthesis. The synthesis of new cryptophanes **2** and **3** was performed by using an experimental procedure slightly modified from that developed by A. Collet and co-workers for the synthesis of known compounds **1** and **4**.[4] A description of the synthetic details and the full characterization of the compounds through high-resolution mass spectrometry, ^{1}H NMR, and ^{13}C NMR spectroscopy are reported in the Supporting Information.

Mass spectra (HRMS, LSIMS) were performed by the Centre de Spectrométrie de Masse, University of Lyon, on a Thermo-Finnigan MAT 95XL spectrometer. ^{1}H and ^{13}C NMR spectra were recorded on Varian Unity$^+$ 500 and Bruker Avance DRX500 spectrometers. Column chromatographic separations were carried out over Merck silica gel 60 (0.040−0.063 mm). Analytical thin-layer chromatography was performed on MERCK silica gel TLC plates F-254. Melting points were measured on a Perkin-Elmer DSC7 calorimeter. The solvents were distilled prior to use: DMF from CaH_2, CH_2Cl_2 from $CaCl_2$, and THF from Na/benzophenone. Cs_2CO_3 was purchased from Acros.

B. NMR Sample Preparation. For the xenon−cryptophane binding experiments, samples of one cryptophane or a mixing of the four cryptophanes were prepared by the following way. The cryptophane powder was weighed on a Sartorius balance (precision: 0.01 mg). After lyophilization and pH adjustment (the pH was adjusted by addition of NaOD between 4.7 and 12.3), a known mass of cryptophane was introduced in 360 μL of D_2O to give total cryptophane concentrations in the range 2−6 mM. The respective experimental errors on the masses and volumes were estimated to be 5 and 3%. Then the samples were degassed by several freeze−pump−thaw cycles.

Laser-polarized xenon was prepared by the spin-exchange method[22] using our apparatus previously described.[23] Xenon in natural abundance comes from Air Liquide and xenon enriched at 96% in isotope 129 from Chemgas. A partial pressure of 2.7 kPa in our pumping cell gave a pressure of ca. 110 kPa in the NMR tube, with an average xenon nuclear polarization of ∼0.25 (measured in the spectrometer magnet). For the experiments using pressure above 10 kPa, frozen laser-polarized xenon was transferred to the NMR tube containing the cryptophane solution thanks to a vacuum line. This operation occurred in the fringe field of the NMR magnet to avoid brutal loss of polarization during xenon sublimation and freezing.[24] For experiments with lower pressure, a direct gas expansion without condensation was performed, the sample being cooled to about 210 K with a methanol bath to strongly reduce the vapor pressure of water. The final pressure in the NMR tube was checked by gas expansion in a vacuum line of known volume equipped with a 0−100 Torr membrane gauge (model Ceramicel from Varian, with a precision of 0.01 Torr). The experimental error on the xenon pressure is estimated to 5%.

C. NMR Acquisition and Processing. NMR experiments involving xenon were performed at 293 K in a 11.7 T magnetic field (^{1}H Larmor frequency = 500.13 MHz; ^{129}Xe Larmor frequency = 138.36 MHz) on a Bruker Avance DRX500 spectrometer. A 5 mm Nalorac broadband direct probehead and a 5 mm Bruker broadband inverse probehead were used. The peak picking, signal integration, and line width measurements were performed using Bruker Xwinnmr3.5 software, or PeakFit software 4.11, distributed by SPSS inc. A precision of 2% on the area of intense and isolated xenon signals was estimated. The xenon chemical shifts were referenced to the signal of xenon in water calibrated at 197 ppm. The 2D ^{1}H EXSY experiments were performed at 274, 288, 298, 303, 313, and 323 K with mixing times ranging from 3 μs to 800 ms. The most isolated spin system of the proton spectrum was chosen for signal integration and processing.

D. Computation of the Xenon Binding Constants. The total number of moles of xenon introduced in the NMR tube was known from the volume of the pumping cell and the pressure of xenon introduced in this cell. As little gas losses could occur during the transfer, the pressure was also measured after the experiment by expanding the xenon from the tube into a vacuum line of known volume equipped with a membrane gauge. The number of moles of free xenon in solution was then deduced from the Ostwald coefficient of xenon in water at the experimental temperature.[25] The solubility of xenon in water depends only slightly upon salinity in our range of ionic strengths.[25] Also, we did not observe any significant effect of the pH (in the 4.7−12.3 range) on the respective binding constant values.

For the first method (determination of the binding constants from the proton spectra), proton spectra with long interscan delays were recorded for 13−15 xenon pressures up to ca. 300 kPa. Two signals characteristic of cryptophane in **CC** conformation were integrated on each spectrum. One signal decreased when gas pressure increased and was therefore assigned to "empty" cryptophanes. The other signal increased with gas pressure and was assigned to cryptophanes filled by a xenon atom. The fraction of one of these integrals was plotted against xenon pressure. The number of xenon moles in the three environments, namely in the gas phase, dissolved in water, and bound to cryptophane, was extracted. The binding constant K was then fitted by the theoretical model of stoichiometry 1:1 against xenon pressure. A reduced χ^2 was calculated and serves to validate the errors on the integrals. Considering the relative errors from 2 to 5% on each experimental parameter, the median K value and the K values at a 90% level of confidence were deduced through Monte Carlo simulation repeated 2000 times.

In the second method (determination of the xenon binding constant from the ^{129}Xe spectra), the proportion of the different crown−crown

(18) Dubois, L.; Parrès, S.; Huber, J. G.; Berthault, P.; Desvaux, H. *J. Phys. Chem. B* **2004**, *108*, 767−773.
(19) Desvaux, H.; Huber, J. G.; Brotin, T.; Dutasta, J.-P.; Berthault, P. *ChemPhysChem* **2003**, *4*, 384−387.
(20) Luhmer, M.; Goodson, B. M.; Song, Y.-Q.; Laws, D. D.; Kaiser, L.; Cyrier, M. C.; Pines, A. *J. Am. Chem. Soc.* **1999**, *121*, 3502−3512.
(21) Kuck, D.; Schuster, A.; Krause, R. A.; Tellenbroker, J.; Exner, C. P.; Penl, K.; Bögge, H.; Muller, A. *Tetrahedron* **2001**, *57*, 3587−3613.
(22) Happer, W.; Miron, E.; Schaefer, S.; Schreiber, D.; van Wijngaarden, W. A.; Zeng, X. *Phys. Rev. A* **1984**, *29*, 3092−3110.
(23) Desvaux, H.; Gautier, T.; Le Goff, G.; Pétro, M.; Berthault, P. *Eur. Phys. J. D* **2000**, *12*, 289−296.
(24) Gatzke, M.; Cates, G. D.; Driehuys, B.; Fox, D.; Happer, W.; Saam, B. *Phys. Rev. Lett.* **1993**, *70*, 690−693.
(25) Clever, H. L. *IUPAC Solubility Data Series*; Pergamon Press: Oxford, 1979.

(**CC**) and crown−saddle (**CS**) cryptophane conformations was first measured using ^{1}H spectra. The number of moles of bound xenon was deduced from the relative area of the two signals on the ^{129}Xe NMR spectrum, i.e., free xenon in water and bound to cryptophane. The number of moles of xenon-free cryptophanes was deduced from the number of moles of cages initially introduced in solution. A binding constant K could then be calculated, assuming a 1:1 model. A Monte Carlo simulation repeated 100 000 times was performed with considering the same experimental errors. Like previously, the median K value and the K values at a 90% level of confidence were deduced.

E. Molecular Modeling. The simulations were performed using CNS 1.1 software[26] under Linux Redhat 7.2. With no topology and parameter files being available for these molecules, they were built step by step. Some parameters, such as bond lengths and angles, partial charges, and nonbonded parameters, were adapted from Kirchhoff et al.[27] The generic topology file was built entirely from scratch. The difference between **CC** and **CS** forms of **1** residing in a dihedral angle around one CH_2 group between two aromatic rings, a specific atom type, was introduced for this carbon in the saddle form with a specific dihedral angle value.

The ring current effects induced by the cyclotriveratrylene moieties were predicted via a simplistic dipolar law of the form $\Delta\delta_i = f\sum_j(1 - 3\cos^2\theta_{ij})r_{ij}^{-3}$, where r_{ij} is the distance between the proton i under consideration and the center of the aromatic ring j, θ_{ij} is the angle between the vector $\vec{r}_{ij}$ and the normal to the aromatic plane j, and f is a proportionality constant.[13] An average shift value over all the accepted structures was computed for each proton.

IV. Conclusions

By replacing the methoxy groups with OCH_2COOH groups, cryptophanes become soluble in water at pH > 5. In the aim of designing new xenon-carrier molecules for biosensing applications on the basis of laser-polarized xenon MRI, these molecules have been studied using ^{1}H and ^{129}Xe NMR. A detailed ^{1}H NMR analysis has revealed peculiar features of these cage molecules in aqueous solution: in addition to the crown−crown conformation, these cryptophanes have been shown to exist under nonsymmetrical conformations in which one of the two cyclotriveratrylene units takes a saddle form. These conformations have been structurally and kinetically characterized. They seem unable to bind xenon, at least for compounds with short linkers (**1**−**3**).

The accuracy of the extracted cryptophane−xenon binding constants is limited by the presence of these noncanonical entities. However, these values have been estimated by two independent methods, exploiting either proton or laser-polarized xenon spectra. The binding constants of the canonical crown−crown conformation of **1**−**4** with xenon are among the highest ever measured for a dissolved noble gas and are higher than the corresponding ones for the organic analogues **6**−**9**. The binding constant value of 6800 M^{-1} for xenon in the modified cryptophane-A at room-temperature constitutes the highest affinity value for a host−guest interaction only based on London and Debye forces in water. These results, together with the longitudinal relaxation time value measured for the noble gas inside the cage of **1** and its increase via partial deuteration, constitute promising elements for a future use of these cryptophanes for biosensing using laser-polarized xenon MRI.

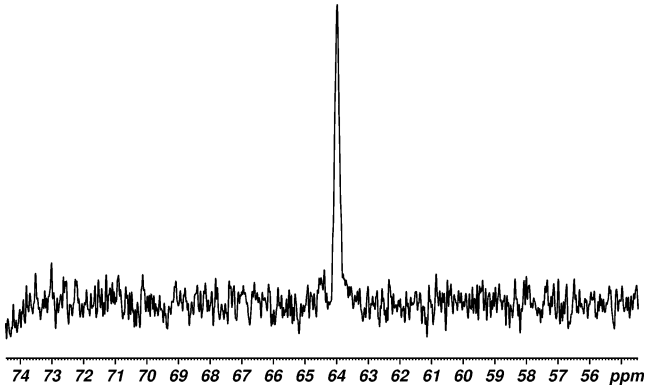

Figure 7. ^{129}Xe NMR spectra of a 1 μM solution of cryptophane **5** in D_2O at 293 K (64 scans, 4 Hz Lorentzian apodization). Xenon pressure: 10.7 kPa. In this experiment, a soft 90° Gaussian pulse of 0.5 ms centered on the signal of xenon in cryptophane has been used to selectively excite this resonance. The exchange with xenon atoms in the solvent (in large excess) maintains the hyperpolarization level at this frequency and enables the use of several scans. Experiment time: 20 s.

The presence of saddle−crown conformers, unable to bind xenon, could represent a limitation to the biosensing approach but could be circumvented in two ways. Either preliminary bubbling could be employed to displace the saddle−crown/crown−crown equilibrium or another synthesis based on blocked cyclotriveratrylene units[21] could be performed. Such structures could avoid the formation of parasitical conformations useless for the transport of xenon.

Thus, grafting of OCH_2COOH groups in place of the methoxy groups on the aromatic rings of cryptophanes seems a good compromise to render these molecules soluble in water at physiological pH while maintaining a high affinity of their cages for xenon. The sharpness of the ^{129}Xe peaks in conditions close to those that will be used in vivo (i.e., low xenon concentration) is an asset for the success of the approach using biosensors based on such cryptophanes. Also, the chemical-shift distribution for xenon inside **1**−**4** should render possible the multiplexed use of such host molecules in chemical-shift MRI applications.

This work thus constitutes a new step toward the use of dedicated cryptophanes for biosensing using laser-polarized xenon MRI. In this approach, in the same way that works have dealt with the adequate choice of the recognition antenna,[28] an in-depth analysis of the cryptophane properties (the architecture of the xenon-carrier molecule) is of importance. Inevitably, the use of such xenon host molecules will encounter some obstacles until final in vivo biosensing applications. Heterogeneous biological media such as blood will contribute more significantly to relaxation than water (but MRI with laser-polarized xenon has already successfully been applied to the study of the brain, for instance[29]), recognition of the antenna could be impeded by the presence of the cryptophane, etc. However, independently of the magnetic field, our polarization level is of 0.25, to be compared to the thermal polarization of ca. 10^{-5} at 11.7 T. Moreover, as there is slow exchange between the signal of free xenon (in water or in blood) and the signal of xenon in cryptophane, the use of low rf power pulses centered around 60 ppm will leave the population of free xenon unaffected and

(26) Brünger, A. T.; Adams, P. D.; Clore, G. M.; DeLano, W. L.; Gros, P.; Grosse-Kunstleve, R. W.; Jiang, J.-S.; Kuszewski, J.; Nilges, M.; Pannu, N. S.; Read, R. J.; Rice, L. M.; Simonson, T.; Warren, G. L. *Acta Crystallogr., Sect. D: Biol. Crystallogr.* **1998**, *54*, 905−921.
(27) Kirchhoff, P. D.; Bass, M. B.; Hanks, B. A.; Briggs, J. M.; Collet, A.; McCammon, J. A. *J. Am. Chem. Soc.* **1996**, *118*, 3237−3246.
(28) Lowery, T. J.; Garcia, S.; Chavez, L.; Ruiz, J. E.; Wu, T.; Brotin, T.; Dutasta, J.-P.; King, D. S.; Schultz, P. G.; Pines, A.; Wemmer, D. E. *ChemBioChem* **2006** *7*, 65−73.
(29) Swanson, S. D.; Rosen, M. S.; Agranoff, B. W.; Coulter, K. P.; Welsh, R. C.; Chupp, T. E. *Magn. Reson. Med.* **1997** *38*, 695−698.

will allow the replenishing of laser-polarized xenon inside the cryptophanes via exchange. Finally, the last argument in favor of this approach lies in the absence of in vivo xenon background, due first to the exogenous nature of this atom, and second to the chemical shift value of xenon in cryptophane, radically different from the chemical shift of xenon in blood or lipids. Obviously, the millimolar concentrations used in our studies are far beyond the concentrations that will be used in in vivo biosensing. To evaluate the sensitivity limit of our approach, an experiment has been performed at room temperature for a cryptophane concentration of 1 μM (Figure 7). After 20 s, the signal-to-noise ratio for xenon in cryptophane is $\sim$16, exemplifying the sensitivity of the approach.

Therefore, these cryptophanes represent a set of candidates for biosensing, affording flexibility in the type of method used for delivering laser-polarized xenon. If, in the first approach, solutions containing the xenon−cryptophanes complexes are designed to be injected, hosts with high xenon affinity will be chosen, whereas if xenon is added in a second step, the in−out exchange rates will become the key parameters.

Acknowledgment. Financial support from the Conseil Général de l′Essonne (ASTRE 2003 program) is acknowledged.

Supporting Information Available: Synthetic details. Figure describing the synthetical scheme. Table and a Figure detailing the ^{1}H and ^{13}C NMR assignment of asymmetrical cryptophanes **2** and **3**. Figure displaying the ^{129}Xe spectrum of an equimolar mixture of cryptophanes **1** and **5**. This material is available free of charge via the Internet at http://pubs.acs.org.

JA060266R